entropy

MDPI

Article

On the Consensus Performance of Multi-Layered MASs with Various Graph Parameters—From the Perspective of Cardinalities of Vertex Sets

Da Huang [1,*] and Zhiyong Yu [2]

[1] Department of Mathematics and Physics, Xinjiang Institute of Engineering, Urumqi 830023, China
[2] College of Mathematics and System Science, Xinjiang University, Urumqi 830017, China
* Correspondence: hd@xjie.edu.cn

Abstract: This work studies the first-order coherence of noisy multi-agent networks with multi-layered structures. The coherence, which is a sort of performance index of networks, can be seen as a sort of measurement for a system's robustness. Graph operations are applied to design the novel multi-layered networks, and a graph spectrum approach, along with analysis methods, is applied to derive the mathematical expression of the coherence, and the corresponding asymptotic results on the performance index have been obtained. In addition, the coherence of these non-isomorphic multi-layered networks with three different graph parameters are compared and analyzed. We find that, when the cardinalities of the vertex sets of corresponding counterpart layers are the same, the multi-layered topology class with a balanced, complete, multi-partite structure has the best robustness of all the considered networks, if the sufficient conditions for the node-related parameters hold. Finally, simulations are given to verify the asymptotic results.

Keywords: multi-agent systems (MASs); consensus; multi-partite graph; multilayered networks; Laplacian spectrum

check for updates

Citation: Huang, D.; Yu, Z. On the Consensus Performance of Multi-Layered MASs with Various Graph Parameters—From the Perspective of Cardinalities of Vertex Sets. *Entropy* **2023**, *25*, 40. https://doi.org/10.3390/e25010040

Academic Editors: Matjaz Perc and Adam Lipowski

Received: 17 October 2022
Revised: 14 December 2022
Accepted: 21 December 2022
Published: 26 December 2022

Copyright: © 2022 by the authors. Licensee MDPI, Basel, Switzerland. This article is an open access article distributed under the terms and conditions of the Creative Commons Attribution (CC BY) license (https://creativecommons.org/licenses/by/4.0/).

1. Introduction

The consensus problem is a significant interdisciplinary field of MASs. It requires that all nodes in the networked system interact with each other based on the communication links and control protocols, so that they can achieve the desired physical states.

Researchers have done lots of significant work on consensus from various perspectives, such as the system order [1–22] (first/higher order or fraction order [7]), patterns of communication (continuous or discontinuous [4,8]), control methods (adaptive control [6–8], intermittent control [9]), and convergence time (finite time or fixed time [5,10]).

In the problem of complex networks, the interactive relationship in the networked system can be always interpreted by the topological structures [22–24], and some performance index of the system, such as consensus speed [1,11] or network coherence [13–21], can be characterized by the second smallest Laplacian eigenvalue or Laplacian spectrum, respectively. Similarly, synchronization problem can also be studied from the aspect of system structures [23–30].

In the past two decades, there has been lots of significant enlightening research on the Laplacian eigenvalues [1,12–22,31–33] of the networked systems. Reference [12] has studied the mathematical relations between the Laplacian eigenvalues and robustness, and derived the H_2 norms of some classic network structures. The robustness of the noisy systems can be defined by network coherence, and the notion was proposed in [13,14]. These articles discovered the fact that the coherence can be characterized by the nonzero Laplacian eigenvalues. Reference [16] studies the robustness of a noisy, scale-free, small-world Koch network, and shows that coherence relies on the shortest-path distance between the lead vertex and the largest-degree vertices. In [19], an analytical expression for the

leader–follower coherence is determined that depends on the numbers of leaders and network parameters.

Recently, multilayered structures became a hot research topic of complex networks [22,25–27,31–33] because of their potential applications. It is natural and meaningful to extend the Laplacian-spectrum approach to the consensus problems with multilayered structures. The multi-partite graph is also a significant structure in many fields, such as heterogeneous networks [28], the field of graph searching [29], and electric networks [30].

Inspired by the above facts, this research considers multi-layered MASs with specific topological structures that are constructed by graph operations. In addition, another sort of multi-layered systems with classic graph as subgraphs are studied for contrast, since they all have a fan shaped structure as their layered graph from the vertical sight. Specifically, the novelties are listed as follows:

I. A sort of novel multi-layered MAS with a balanced, complete, multi-partite graph has been constructed by graph operations. Different from other good research on multilayered coordination systems, the side structure in this article from the vertical view has the fan-shaped structure.
II. Analysis methods with various parameters are applied for deriving the coherence, and the related asymptotic properties have been acquired.
III. We found that when the vertex sets of the corresponding counterpart layers have the same cardinality, the multi-layered graph class with a complete multi-partite structure has the best robustness of all the considered layered systems if the sufficient conditions for the parameters hold.

The aims for this paper were to study the robustness related index of the multi-layer MAS with noise and determine the mathematical expression for the coherence, and to further calculate the corresponding limitation-related results.

In Section 2, the needed notation of graph theory is explained, and the mathematical relation for the Laplacian eigenvalues and the coherence is described. Section 3 describes the topological structures of the multi-layered networks, and the derivations for the coherence are given. The simulated results are presented in Section 4.

2. Preliminaries

2.1. Graph Theory and Notations

Denote the complete graph with n vertices by K_n, and the star graph with $k-1$ leaf vertices is represented as S_k. $\mathfrak{E}_k$ denotes the empty graph with k vertices. Denote the fan graph with q vertices by F_q. Let G be a graph with vertex set $V = \{v_1, v_2, \ldots, v_N\}$, and its edge set is defined as $\mathcal{E} = \{(v_i, v_j)|i, j = 1, 2, \ldots, N; i \neq j\}$ The adjacency matrix is defined as $A(G) = [a_{ij}]_N$, where a_{ij} is the weight of (v_i, v_j). This paper considers the undirected graph, in which the edge weight satisfies: $a_{ij} = a_{ji}$, and it is supposed that $a_{ij} = 1$, if $(v_i, v_j) \in \mathcal{E}; a_{ij} = 0$, if $(v_i, v_j) \notin \mathcal{E}$. The Laplacian matrix of G is denoted as $L(G) = D(G) - A(G)$, where $D(G)$ is defined by $D(G) = diag(d_1, d_2, \ldots, d_N)$ with $d_i = \sum_{j \neq i} a_{ij}$. The Laplacian spectrum of G is denoted by $SL(G) = \begin{pmatrix} \lambda_1(G) & \lambda_2(G) & ... & \lambda_p(G) \\ l_1 & l_2 & ... & l_p \end{pmatrix}$, where $\lambda_1(G) < \lambda_2(G) < ... < \lambda_p(G)$ are the Laplacian eigenvalues, and $l_1, l_2, \ldots, l_p$ are the multiplicities of the eigenvalues [34].

In addition, the following definitions and lemmas are needed for deriving the results.

Definition 1 ([28–30]). *Let $\mathfrak{K}_{n_1,n_2,\ldots,n_k} = (V_1, \ldots, V_k, E)$ be the complete multi-partite graph, where $V_1, \ldots, V_k$ are disjoint vertex sets, $|V_i| = n_i$, and $1 \leq i \leq k$; each vertex in V_i is adjacent to all the vertices in $V(\mathfrak{K}_{n_1,\ldots,n_k}) \setminus V_i$. In particular, when $n_i = s$, it is called a balanced complete multi-partite graph, and we denote it by $\mathfrak{K}(k, m)$.*

Definition 2 ([35,36]). *(The Cartesian product of two graphs) For two graphs $G_1 = (V_1, E_1)$ and $G_2 = (V_2, E_2)$, the Cartesian product graph $G = G_1 \times G_2$ is the graph with vertex set $V_1 \times V_2$. There is an edge from the vertex (x_1, y_1) to the vertex (x_2, y_2) if and only if either $x_1 = x_2$ and $y_1, y_2 \in E_2$ or $y_1 = y_2$ and $x_1, x_2 \in E_1$.*

Definition 3 ([35]). *(The join of two graphs) The join of simple graphs G_1 and G_2, written $G_1 \triangledown G_2$, is the graph obtained from the disjoint union of G_1 and G_2 by adding the edges $\{xy : x \in V(G_1), y \in V(G_2)\}$.*

Definition 4 ([37,38]). *(The corona of two graphs) Let G_1 and G_2 be two graphs on disjoint sets of n and k vertices, respectively. The corona $G_1 \circ G_2$ of G_1 and G_2 is defined as the graph obtained by taking one copy of G_1 and n copies of G_2, and then joining the ith vertex of G_1 to every vertex in the ith copy of G_2, $(i = 1, 2, \ldots, n)$.*

Lemma 1 ([34]). *If G_1 has m vertices and G_2 has n vertices, then the Laplacian eigenvalues of $G_1 \times G_2$ are the mn numbers: $\nu_i(G) + \nu_j(H)$ $(i = 1, 2..., m;\ j = 1, 2, \ldots, n)$, where $\nu_i(G)$ and $\nu_j(H)$ are the Laplacian eigenvalues of G_1 and G_2, respectively.*

Lemma 2 ([34]). *If G_1 has m vertices and G_2 has n vertices, then the Laplacian eigenvalues of $G_1 \triangledown G_2$ are: $0, m + n, m + \lambda_i, n + \mu_j, i = 2, 3, \ldots, n;\ j = 2, 3, \ldots, m$, where λ_i and μ_j are the non-zero Laplacian eigenvalues of G_1 and G_2, respectively.*

2.2. Relations for the Coherence and Laplacian Eigenvalues

Refer to references [13–17]. This article considers the first-order noisy network:

$$\dot{x}(t) = -L(G)x(t) + \xi(t), \tag{1}$$

where $x \in R^N$, and $\xi(t) \in R^N$ is a disturbance vector with zero-mean, unit variance, and a white stochastic noise process.

Definition 5 ([13,14]). *The first-order network coherence is defined as the mean steady-state variance of the deviation from the average of all node states:*

$$H = \lim_{t\to\infty} \frac{1}{N} \sum_{i=1}^{N} Var\left\{ x_i(t) - \frac{1}{N} \sum_{j=1}^{N} x_j(t) \right\}.$$

Denote the Laplacian eigenvalues of G by $0 = \lambda_1 < \lambda_2 \leq \ldots \leq \lambda_N$. It has been proved that H can be characterized by

$$H = \frac{1}{2N} \sum_{i=2}^{N} \frac{1}{\lambda_i}. \tag{2}$$

The performance index has some similarity with the resistance distance [15,39,40] and Kirhoff index [39–41], and other graphical indices [42,43] related to topological structures.

3. Main Results

The multilayered networked systems own the graphs composed by connecting the corresponding counterpart nodes of different layers. The following subsections propose the fan-graph-based multilayered structures, starting from the perspective of the multi-partite graph, and then deriving and comparing the first-order coherence of the noisy MASs.

3.1. The Coherence for Network Topology $\mathbb{G}_1(a, m, q)$

In this subsection, a class of multiplex networks with complete multi-partite structure is considered. The topology can be generated by the operation of complete k-partite graph and fan-graph. Define $\mathbb{G}_1(a, m, q) := \Re(a, m) \times F_q$, and denote the corresponding network

with dynamics (1) by $\mathfrak{G}_1$. As shown in Figure 1, from the side view, it has the fan graph structure, and from the horizontal view, each layer is a complete bipartite graph with the partition number $a = 2$, and each partition set has two nodes in it; i.e., $m = 2$. The layer in which each node has the largest vertex degree is named the center layer (see Figure 1), and the vertices in this layer can be viewed as the hub node of the fan graph from the vertical view.

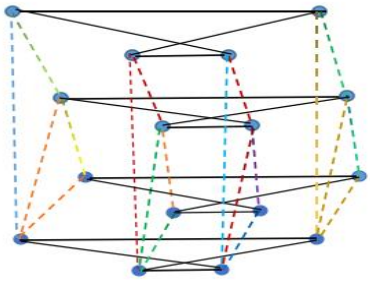


Figure 1. An example of $\mathbb{G}_1(a, m, q)$ with $a = 2, m = 2, q = 4$.

By Lemma 2, one has

$SL[\mathfrak{K}(a,m)] = \begin{pmatrix} 0 & am & (a-1)m \\ 1 & a-1 & am-a \end{pmatrix}$, and since

$SL(F_q) = \begin{pmatrix} 0 & q & 1+4sin^2(\frac{k\pi}{2(q-1)}) \\ 1 & 1 & q-2 \end{pmatrix}$.

By Lemma 1, it can be derived that $SL[\mathbb{G}_1(a, m, q)]$ has the description:

(1). $0 \in SL[\mathbb{G}_1(a, m, q)]$ with multiplicity 1;
(2). $am \in SL(\mathbb{G}_1(a, m, q))$ with multiplicity $(a-1)$;
(3). $(a-1)m \in SL(\mathbb{G}_1(a, m, q))$ with multiplicity $a(m-1)$;
(4). $q \in SL(\mathbb{G}_1(a, m, q))$ with multiplicity 1;
(5). $q + am \in SL(\mathbb{G}_1(a, m, q))$ with multiplicity $a-1$;
(6). $q + (a-1)m \in SL(\mathbb{G}_1(a, m, q))$ with multiplicity $a(m-1)$;
(7). $1 + 4sin^2\frac{k\pi}{2(q-1)} \in SL(\mathbb{G}_1(a, m, q))$ with multiplicity 1, where $k = 1, 2, \ldots, q-2$;
(8). $am + 1 + 4sin^2\frac{k\pi}{2(q-1)} \in SL(\mathbb{G}_1(a, m, q))$ with multiplicity $a-1$, $k = 1, 2, \ldots, q-2$;
(9). $(a-1)m + 1 + 4sin^2\frac{k\pi}{2(q-1)} \in SL(\mathbb{G}_1(a, m, q))$ with multiplicity $a(m-1)$, $k = 1, 2, \ldots, q-2$.

Therefore, we have

$$\begin{aligned} H^{(1)}(\mathfrak{G}_1) =& \frac{1}{2amq}\Bigg((a-1)\frac{1}{am} + (am-a)\frac{1}{(a-1)m} + \frac{1}{q} + (a-1)\frac{1}{q+am} \\ &+ (am-a)\frac{1}{q+(a-1)m} + \sum_{k=1}^{q-2}\frac{1}{1+4sin^2\frac{k\pi}{2(q-1)}} \\ &+ (a-1)\sum_{k=1}^{q-2}\frac{1}{am+1+4sin^2\frac{k\pi}{2(q-1)}} + (am-a)\sum_{k=1}^{q-2}\frac{1}{(a-1)m+1+4sin^2\frac{k\pi}{2(q-1)}}\Bigg). \end{aligned}$$

(i). If $a,\ m$ are fixed, let $q \to \infty$, then one can get that:

$$\lim_{q\to\infty} H(\mathfrak{G}_1) = \frac{\sqrt{5}}{10am} + \frac{(a-1)}{2am\sqrt{(am+5)(am+1)}} + \frac{(am-a)}{2am\sqrt{[(a-1)m+5][(a-1)m+1]}},$$

and hence, by contraction of inequality, when a is large enough, $H(\mathfrak{G}_1) \to 0$; when m is large enough, $H(\mathfrak{G}_1) \to 0$.

(ii). If a, q are fixed, let $m \to \infty$. Then, $H(\mathfrak{G}_1) \to 0$.

(iii). Suppose that m, q are fixed, let $a \to \infty$, and then $H(\mathfrak{G}_1) \to 0$ also holds.

3.2. The Coherence for Network Topology $\mathbb{G}_2(n,p,q)$

As shown in Figure 2, from the horizontal vision, each layer is composed by the join of the complete graph and the empty graph. The complete subgraph can be viewed as a generation of the concept of the hub node of a star graph. From the side view, it can be seen as the fan graph structures. Mathematically, define $\mathbb{G}_2(n,p,q) := (K_n \triangledown E_p) \times F_q$, and the corresponding noisy network is denoted by $\mathfrak{G}_2$. It can be derived that the Laplacian spectrum has the following characterization:

(1). $0 \in SL[\mathbb{G}_2(n,p,q)]$ with multiplicity 1;
(2). $n+p \in SL[\mathbb{G}_2(n,p,q)]$ repeated n times;
(3). $n \in SL[\mathbb{G}_2(n,p,q)]$ repeated $p-1$ times;
(4). $q \in SL[\mathbb{G}_2(n,p,q)]$ with multiplicity 1;
(5). $n+p+q \in SL[\mathbb{G}_2(n,p,q)]$ with multiplicity n;
(6). $n+q \in SL[\mathbb{G}_2(n,p,q)]$ repeated $p-1$ times;
(7). $1+4sin^2(\frac{k\pi}{2(q-1)}) \in SL[\mathbb{G}_2(n,p,q)]$ with multiplicity 1, $k = 1,2,\ldots,q-2$;
(8). $n+p+1+4sin^2(\frac{k\pi}{2(q-1)}) \in SL[\mathbb{G}_2(n,p,q)]$ with multiplicity n, $k = 1,2,\ldots,q-2$;
(9). $n+1+4sin^2(\frac{k\pi}{2(q-1)}) \in SL[\mathbb{G}_2(n,p,q)]$ repeated $p-1$ times, $k = 1,2,\ldots,q-2$.

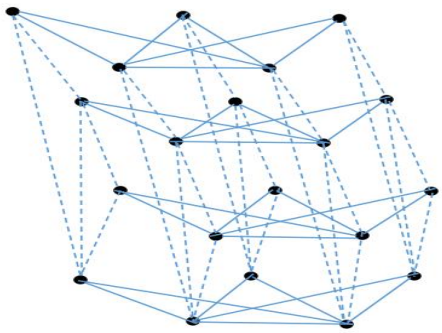


Figure 2. An example of $\mathbb{G}_2(n,p,q)$ with $n = 2, p = 3, q = 4$.

Therefore,

$$\begin{aligned} H(\mathfrak{G}_2) =& \frac{1}{2(n+p)q}\Big[\frac{n}{n+p} + \frac{p-1}{n} + \frac{1}{q} + \frac{n}{n+p+q} + \frac{p-1}{n+q} + \sum_{k=1}^{q-2}\frac{1}{1+4sin^2(\frac{k\pi}{2(q-1)})} \\ &+ n\sum_{k=1}^{q-2}\frac{1}{n+p+1+4sin^2(\frac{k\pi}{2(q-1)})} + (p-1)\sum_{k=1}^{q-2}\frac{1}{n+1+4sin^2(\frac{k\pi}{2(q-1)})}\Big]. \end{aligned}$$

Thus, we have,
(i).

$$\begin{aligned} \lim_{q\to\infty} H(\mathfrak{G}_2) =& \frac{1}{2(n+p)}\int_0^1 \frac{1}{1+4sin^2(\frac{\pi x}{2})}dx + \frac{n}{2(n+p)}\int_0^1 \frac{1}{n+p+1+4sin^2(\frac{\pi x}{2})}dx \\ &+ \frac{p-1}{2(n+p)}\int_0^1 \frac{1}{n+1+4sin^2(\frac{\pi x}{2})}dx \\ =& \frac{\sqrt{5}}{10(n+p)} + \frac{n}{2(n+p)}\frac{1}{\sqrt{(n+p+5)(n+p+1)}} + \frac{p-1}{2(n+p)}\frac{1}{\sqrt{(n+5)(n+1)}} \end{aligned}$$

(ii). When $p \to \infty$, $H(\mathfrak{G}_2) \to \frac{1}{2nq} + \frac{1}{2(n+q)q} + \frac{1}{2q}\sum_{k=1}^{q-2}\frac{1}{n+1+4sin^2\frac{k\pi}{2(q-1)}}$;
(iii). When $n \to \infty$, $H(\mathfrak{G}_2) \to 0$.

Remark 1. *If the numbers of vertices of each layer of* $\mathfrak{G}_1$ *and* $\mathfrak{G}_2$ *are equal, that is,* $am = n + p$*, then the sufficient condition that makes* $\lim_{q\to\infty} H(\mathfrak{G}_1) \geq \lim_{q\to\infty} H(\mathfrak{G}_2)$ *hold is acquired:* $\frac{n+p-a}{n+p-m+5} \geq \frac{p-1}{n+1}$*, where* $a, m, n, p \geq 2$*, and the parameters are all integer.*

3.3. The Coherence of Structure $\mathbb{G}_3(n, q, l)$

In this case, a class of multi-layered star-composed structure is considered. Each layer can be viewed as several star-shaped copies formed into the complete subgraph by the center vertices (see Figure 3), and all layers are connected only through black counterpart nodes. It can be seen as the fan graph from the side view perspective. Define $\mathbb{G}_3(n, q, l) = (K_n \times F_q) \circ E_l$, and denote the corresponding noisy network by $\mathfrak{G}_3$.

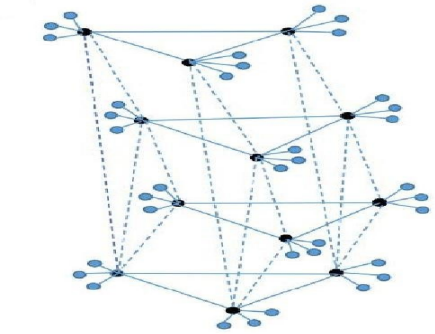


Figure 3. An example of $\mathbb{G}_3(n, q, l)$ with $n = 3, q = 4, l = 3$.

Since

$$SL(K_n \times F_q) = \begin{pmatrix} 0 & q & 1+4sin^2\frac{k\pi}{2(q-1)} & n & n+q & n+1+4sin^2\frac{k\pi}{2(q-1)} \\ 1 & 1 & 1 & n-1 & n-1 & n-1 \end{pmatrix},$$

where $k = 1, 2, \ldots, q-2$.

$SL[\mathbb{G}_3(n, q, l)]$ has the following characterization:

(1). 0 and $l + 1 \in SL[\mathbb{G}_3(n, q, l)]$ repeated once;

(2). $\frac{q+l+1\pm\sqrt{(q+l+1)^2-4q}}{2} \in SL[\mathbb{G}_3(n, q, l)]$ with multiplicity 1;

(3). $\frac{(1+4sin^2\frac{k\pi}{2(q-1)}+l+1)\pm\sqrt{(1+4sin^2\frac{k\pi}{2(q-1)}+l+1)^2-4(1+4sin^2\frac{k\pi}{2(q-1)})}}{2} \in SL[\mathbb{G}_3(n, q, l)]$ repeated once, where $k = 1, 2, \ldots, q-2$.

(4). $\frac{n+l+1\pm\sqrt{(n+l+1)^2-4n}}{2} \in SL[\mathbb{G}_3(n, q, l)]$ repeated $n-1$ times;

(5). $\frac{n+q+l+1\pm\sqrt{(n+q+l+1)^2-4(n+q)}}{2} \in SL[\mathbb{G}_3(n, q, l)]$ repeated $n-1$ times;

(6). $\frac{(n+1+4sin^2\frac{k\pi}{2(q-1)}+l+1)\pm\sqrt{(n+1+4sin^2\frac{k\pi}{2(q-1)}+l+1)^2-4(n+1+4sin^2\frac{k\pi}{2(q-1)})}}{2} \in SL[\mathbb{G}_3(n, q, l)]$ repeated $n-1$ times, where $k = 1, 2, \ldots, q-2$.

(7). $1 \in SL[\mathbb{G}_3(n, q, l)]$ repeated $qn(l-1)$ times.

Therefore,

$$H(\mathfrak{G}_3) = \frac{1}{2nq(1+l)}\Bigg(\frac{1}{l+1} + \frac{q+l+1}{q} + \sum_{k=1}^{q-2}\Big(1 + \frac{l+1}{1+4sin^2\frac{k\pi}{2(q-1)}}\Big) + \frac{(n+l+1)(n-1)}{n} + \frac{(n+q+l+1)(n-1)}{n+q} + \sum_{k=1}^{q-2}\frac{(n+1+4sin^2\frac{k\pi}{2(q-1)}+l+1)(n-1)}{n+1+4sin^2\frac{k\pi}{2(q-1)}} + qn(l-1)\Bigg),$$

and then we have

(i). When $q \to \infty$, $H(\mathfrak{G}_3) \to \frac{1}{2n}\int_0^1 \frac{1}{1+4sin^2\frac{\pi x}{2}}dx + \frac{n-1}{2n}\int_0^1 \frac{1}{n+1+4sin^2\frac{\pi x}{2}}dx + \frac{l}{2(1+l)} = \frac{\sqrt{5}}{10n} + \frac{n-1}{2n}\frac{1}{\sqrt{(n+5)(n+1)}} + \frac{l}{2(1+l)}$;

(ii). When $n \to \infty$, $H(\mathfrak{G}_3) \to \frac{l}{2(1+l)}$;
(iii). When $l \to \infty$,
$H(\mathfrak{G}_3) \to \frac{1}{2nq^2} + \frac{1}{2nq}\sum_{k=1}^{q-2} \frac{1}{1+4sin^2\frac{k\pi}{2(q-1)}} + \frac{n-1}{2n^2q} + \frac{n-1}{2nq(n+q)} + \frac{1}{2nq}\sum_{k=1}^{q-2} \frac{n-1}{n+1+4sin^2\frac{k\pi}{2(q-1)}}$.

Remark 2. *Both $\mathfrak{G}_2$ and $\mathfrak{G}_3$ have the complete substructure K_n, and the number of layers in both cases is q. If the node numbers of one layer in $\mathfrak{G}_2$ and $\mathfrak{G}_3$ are equal, i.e., $n + nl = n + p$, that is, $nl = p$, it can be derived that $\lim_{q\to\infty} H(\mathfrak{G}_3) > \lim_{q\to\infty} H(\mathfrak{G}_2)$ holds.*

3.4. The Coherence for Special Cases

The Laplacian spectrum of star graph with p vertices is:
$SL(S_p) = \begin{pmatrix} 0 & p & 1 \\ 1 & 1 & p-2 \end{pmatrix}$,

Def. $W_1 = S_p \times F_n$, and the related noisy network is denoted by $\mathfrak{W}_1$; then we have $SL(W_1)$

$$= \begin{pmatrix} 0 & n & 1+4sin^2(\frac{k\pi}{2(n-1)}) & p & p+n & p+1+4sin^2(\frac{k\pi}{2(n-1)}) & 1 & 1+n & 2+4sin^2(\frac{k\pi}{2(n-1)}) \\ 1 & 1 & 1 & 1 & 1 & 1 & p-2 & p-2 & p-2 \end{pmatrix}$$

where $k = 1, 2, \ldots, n-2$.

The first-order coherence for network $\mathfrak{W}_1$:

$$\begin{aligned} H(\mathfrak{W}_1) =& \frac{1}{2np}\left(\frac{1}{n} + \sum_{k=1}^{n-2} \frac{1}{1+4sin^2(\frac{k\pi}{2(n-1)})} + \frac{1}{p} + \frac{1}{p+n} + \sum_{k=1}^{n-2} \frac{1}{p+1+4sin^2(\frac{k\pi}{2(n-1)})}\right. \\ &\left. + (p-2) + \frac{p-2}{1+n} + (p-2)\sum_{k=1}^{n-2} \frac{1}{2+4sin^2(\frac{k\pi}{2(n-1)})}\right), \end{aligned}$$

thus,

$$\begin{aligned} \lim_{n\to\infty} H^{(1)} =& \frac{1}{2p}\int_0^1 \frac{1}{1+4sin^2(\frac{\pi x}{2})}dx + \frac{1}{2p}\int_0^1 \frac{1}{p+1+4sin^2(\frac{\pi x}{2})}dx + \frac{p-2}{2p}\cdot\frac{\sqrt{3}}{6} \\ =& \frac{\sqrt{5}}{10p} + \frac{1}{2p}\frac{1}{\sqrt{(p+5)(p+1)}} + \frac{p-2}{2p}\cdot\frac{\sqrt{3}}{6} \end{aligned}$$

Define a noisy network $\mathfrak{W}_2$ with the graph $W_2 := K_p \times F_n$; then we have

$$SL(W_2) = \begin{pmatrix} 0 & n & 1+4sin^2(\frac{k\pi}{2(n-1)}) & p & p+n & p+1+4sin^2(\frac{k\pi}{2(n-1)}) \\ 1 & 1 & 1 & p-1 & p-1 & p-1 \end{pmatrix}$$

where $k = 1, 2, \ldots, n-2$.
Therefore,

$$\begin{aligned} H(\mathfrak{W}_2) =& \frac{1}{2np}\left(\frac{1}{n} + \sum_{k=1}^{n-2} \frac{1}{1+4sin^2(\frac{k\pi}{2(n-1)})} + \frac{p-1}{p} + \frac{p-1}{p+n}\right. \\ &\left. + (p-1)\sum_{k=1}^{n-2} \frac{1}{p+1+4sin^2(\frac{k\pi}{2(n-1)})}\right). \end{aligned}$$

Then one has

$$\lim_{n\to\infty} H(\mathfrak{W}_2) = \frac{1}{2p}\int_0^1 \frac{1}{1+4sin^2(\frac{\pi x}{2})}dx + \frac{p-1}{2p\sqrt{(p+5)(p+1)}}$$
$$= \frac{\sqrt{5}}{10p} + \frac{p-1}{2p\sqrt{(p+5)(p+1)}}$$

Remark 3. *From the above derivation, it can be acquired that* $H(\mathfrak{W}_1) \to \frac{\sqrt{3}}{12}$*, as p is large enough, and* $H(\mathfrak{W}_2) \to 1$ *as p is large enough. For the comparison of the three networks, suppose that* $am = p$*; i.e., the vertex sets of counterpart layers have the same cardinality. In real networks that may have the multi-partite layered structures, one reasonable hypothesis is that* $p \to +\infty$*, usually corresponding to the trend that one of the parameters a and m tends to infinity.*

Remark 4. *The implication of this research is that the mathematical expression of coherence can be a reference for deriving the robustness of similar MASs with multi-layered structures. The asymptotic results has practical significance to improving the robustness of the related network. In addition, the fan-graph from the vertical view, which forms a center layer structurally, might enlighten the future research on the topological design of multi-layer networks.*

4. Simulation and Comparison

This section presents the simulation and comparisons of the coherence for these multi-layered MASs. Figure 4 shows the changes in the coherence with the parameters a and q. These results coincide with the results that Section 3.1 shows; i.e., if m is fixed, then $H(\mathfrak{G}_1) \to 0$ as $q, a \to \infty$. It coincides with results (i) and (iii) in Section 3.1. In Figure 5, the surface is for $H(\mathfrak{G}_1)$ with the changes in m and q, when $a = 3$. The figure implies that $H(\mathfrak{G}_1) \to 0$ as $m \to \infty$, which satisfies results (i) and (ii) in Section 3.1. Figure 6 shows the changes in coherence of $\mathfrak{G}_1$ and $\mathfrak{G}_2$ with the changing of parameter q, i.e., the number of layers; the node related parameters were chosen as: $a = 3, m = 8, n = 18$, and $p = 6$. These satisfy the condition that Remark 2 mentioned: $\frac{n+p-a}{n+p-m+5} \geq \frac{p-1}{n+1}$. One can see that $H(\mathfrak{G}_1)$ is a bit larger than $H(\mathfrak{G}_2)$ in the range of all q, which satisfies the previous result. Figure 7 shows the changes in $H(\mathfrak{G}_2)$ and $H(\mathfrak{G}_3)$ with q, when the other parameters were chosen as $n = 3, l = 3, p = nl = 9$. Figure 8 describes the variation in $H(\mathfrak{G}_1)$ with m, when $a = 3, q = 4$. From the point (197, 0.001469) and the decreasing trend of the curve, one can see that when $m \to \infty$, the coherence $H(\mathfrak{G}_1) \to 0$ coincides with the result in Section 3.1. In Figure 9, the point (194, 0.001072) and the curve reflect the change trends of $H(\mathfrak{G}_1)$ with a, when $m = 3, q = 4$; that is, $H(\mathfrak{G}_1) \to 0$. This also coincides with the previous result. Figure 10 describes the monotonous increasing trend of $H(\mathfrak{G}_2)$ with p. From the former section, we know that when n and q are fixed, $H(\mathfrak{G}_2)$ will tend to a certain value, and the point (196, 0.101) satisfies the result. This coincides with the figure's description. In Figure 11, the curve and the point (191, 0.003161) shows the trend that $H(\mathfrak{G}_2)$ monotonously decreases to 0 when $n \to \infty$. Figure 12 implies the decreasing trend that $H(\mathfrak{G}_3)$ will tend to a certain value when $n \to \infty$, and the certain fixed value is related only to l. In this figure, $q = 4, l = 3$; the point $(193, 0.3781)$ coincides with the result that the former section derived. In Figure 13, the increasing curve implies the trend that $H(\mathfrak{G}_3)$ will tend to a certain value which is related to n and q; at $l \to \infty$, the point (196, 0.6072) is consistent with this fact. One can see that the points on the curves satisfy both the mathematical expression of coherence and the asymptotic results. The simulations also verified the size relation of the three cases when the corresponding layers have the same number of nodes. In summary, the mathematical expression results, the integral calculations, and the simulation with partially fixed parameters are consistent.

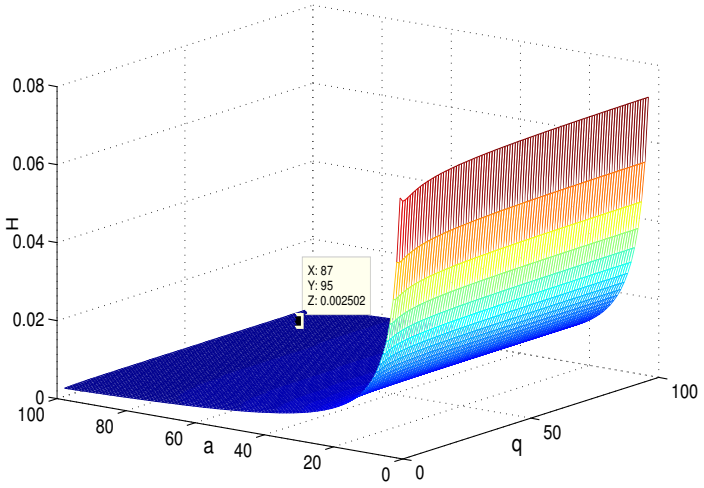


Figure 4. The change in $H(\mathfrak{G}_1)$ with a and q; $m = 3$.

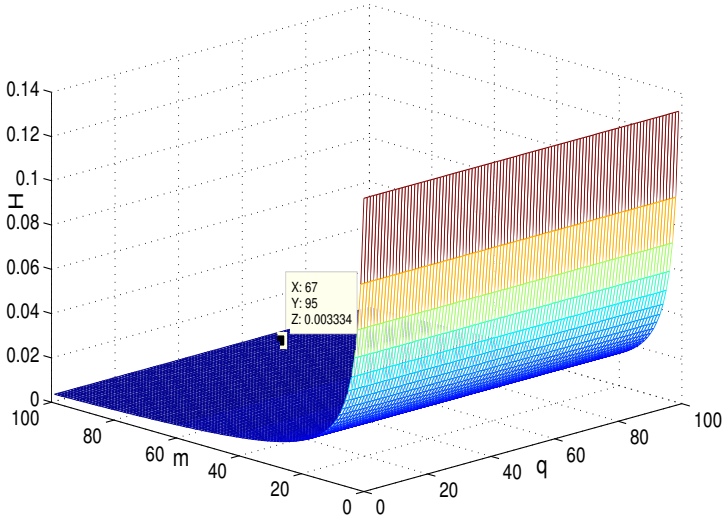


Figure 5. The change in $H(\mathfrak{G}_1)$ with m and q; $a = 3$.

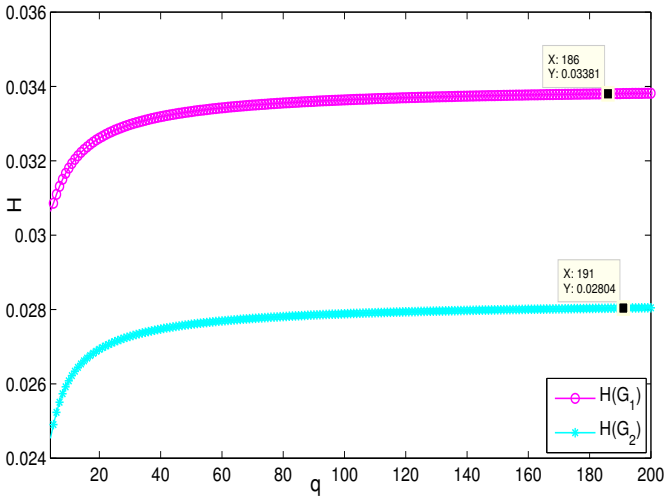


Figure 6. The change in $H(\mathfrak{G}_1)$ and $H(\mathfrak{G}_2)$ with q; $a = 3, m = 8, n = 18, p = 6$.

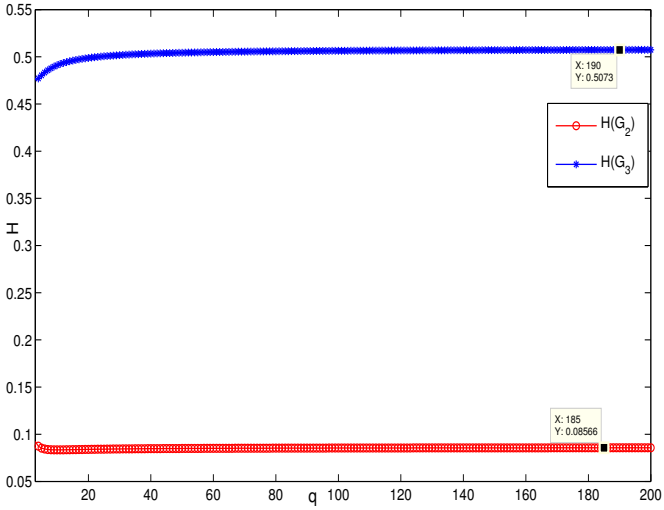


Figure 7. The change in $H(\mathfrak{G}_2)$ and $H(\mathfrak{G}_3)$ with q; $n = 3, l = 3, p = 9$.

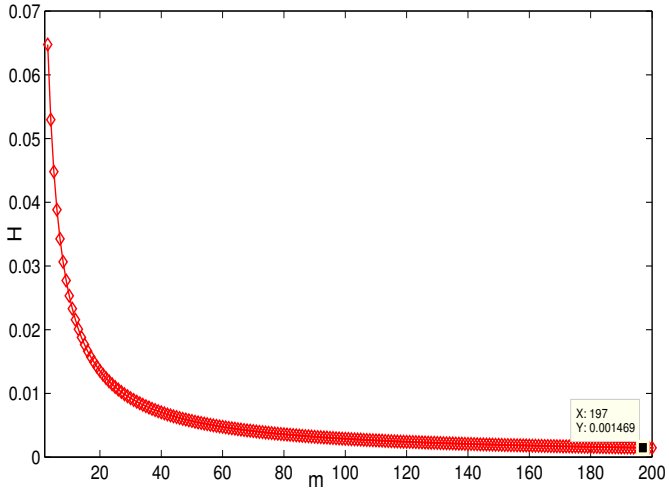


Figure 8. The change in $H(\mathfrak{G}_1)$ with m. $a = 3, q = 4$.

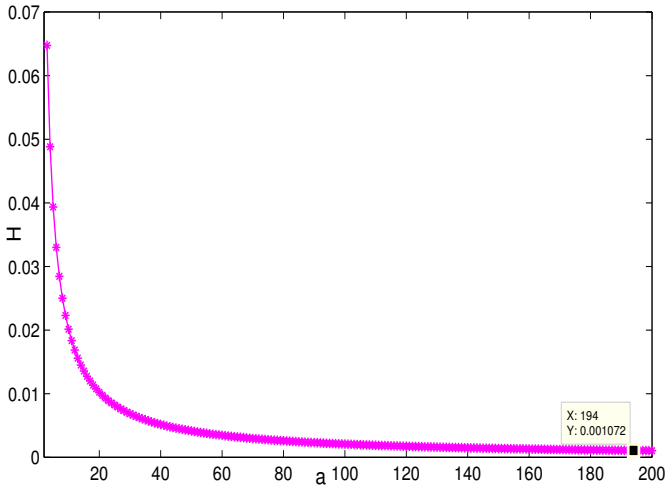


Figure 9. The change in $H(\mathfrak{G}_1)$ with a. $m = 3, q = 4$.

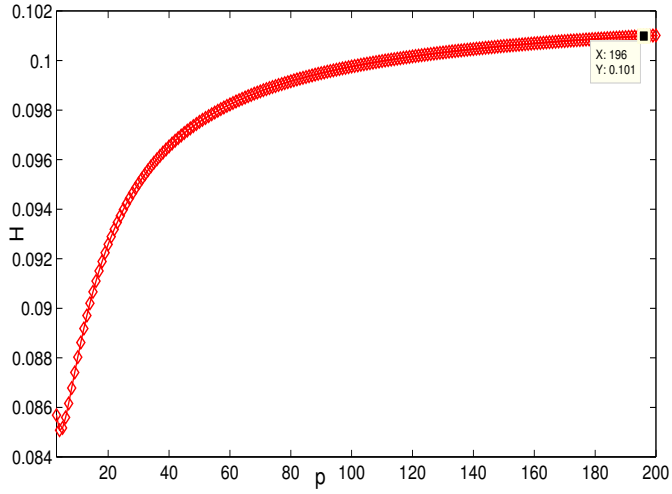


Figure 10. The change in $H(\mathfrak{G}_2)$ with p. $n = 3, q = 4$.

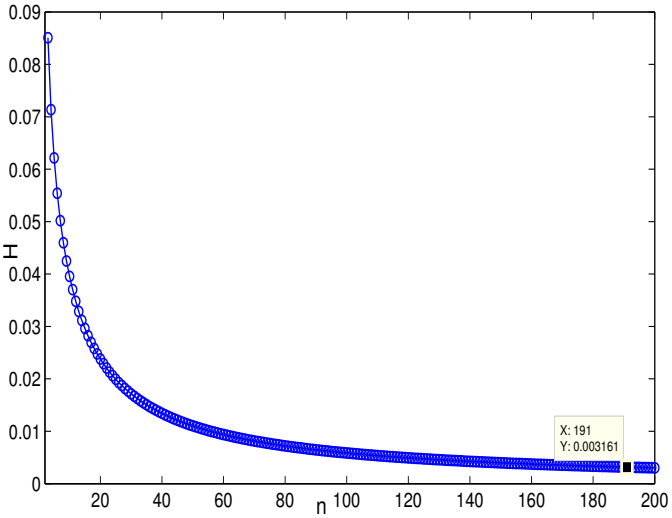


Figure 11. The change in $H(\mathfrak{G}_2)$ with n. $p = 4, q = 4$.

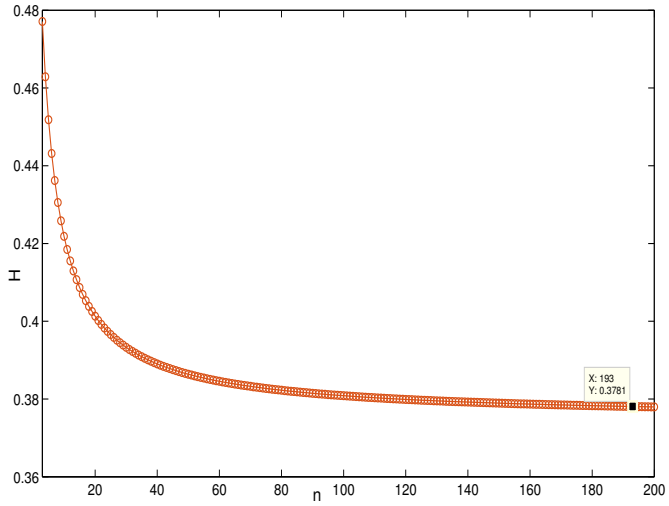


Figure 12. The change in $H(\mathfrak{G}_3)$ with n. $q = 4, l = 3$.

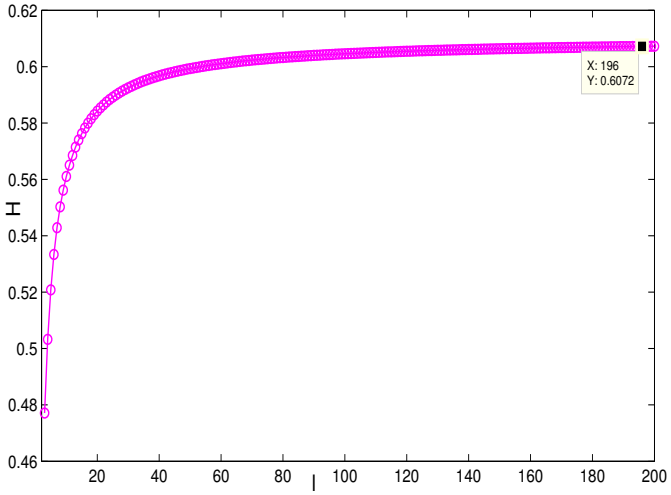


Figure 13. The change in $H(\mathfrak{G}_3)$ with l. $n = 3, q = 4$.

5. Conclusions

In this research, the first-order coherence for several multi-layered MASs with complete, multi-partite graph structures was studied. A fan graph was used to define the novel multi-layered structures. The view from the side perspective shows that each has the fan-graph structure. The approaches of analysis and graph spectra were combined to derive the mathematical expression of a performance index, and the corresponding asymptotic properties have been acquired. We find that when the cardinality of a node set of corresponding counterpart network layers is consistent, the multi-layered topology class with complete multi-partite structure has the best robustness of all the considered systems, if the sufficient conditions for the parameters hold. Finally, the coherence of the non-isomorphic multi-layered networks with the same number of nodes in their counterpart layers were simulated to verify the results.

Author Contributions: Methodology: D.H.; software: D.H. and Z.Y.; validation: D.H. and Z.Y.; formal analysis: D.H.; writing—original draft preparation: D.H.; writing—review and editing: D.H.; supervision: Z.Y.; project administration: D.H. and Z.Y. All authors have read and agreed to the published version of the manuscript.

Funding: This work was supported by the Natural Science Foundation of Xinjiang (NSFXJ) (No. 2019D01B10), the National Natural Science Foundation of Peoples Republic of China (NSFC) (Grants No. 62003289).

Institutional Review Board Statement: Not applicable.

Data Availability Statement: Not applicable.

Acknowledgments: We express our sincere gratitude to the people who gave us valuable comments and thank Cheng Yan, who works at the College of Mathematics and Systems Science, Xinjiang University, for the good advice.

Conflicts of Interest: The authors declare that they have no conflict of interest.

References

1. Saber, O.; Murray, R. Consensus problems in Networks of Agents With Switching Topology and Time-Delays. *IEEE Trans. Autom. Control* **2004**, *49*, 1520–1533. [CrossRef]
2. Ren, W. On consensus algorithms for double-integrator dynamics. *IEEE Trans. Autom. Control* **2008**, *53*, 1503–1509. [CrossRef]
3. Yu, W.; Chen, G.; Cao, M.; Kurths, J. Second-order consensus for multiagent systems with directed topologies and nonlinear dynamics. *IEEE Trans. Syst. Man Cybern.-Part Cybern.* **2010**, *40*, 881–891.
4. Wen, G.; Duan, Z.; Yu, W.; Chen, G. Consensus of second-order multi-agent systems with delayed nonlinear dynamics and intermittent communications. *Int. J. Control* **2013**, *86*, 322–331. [CrossRef]
5. Shang, Y. Finite-time Consensus for Multi-Agent Systems with Fixed Topologies. *Int. J. Syst. Sci.* **2012**, *43*, 499–506. [CrossRef]

6. Yu, Z.; Huang, D.; Jiang, H.; Hu, C.; Yu, W. Distributed consensus for multiagent systems via directed spanning tree based adaptive control. *Siam Control. Optim.* **2018**, *56*, 2189–2217. [CrossRef]
7. Yu, Z.; Jiang, H.; Hu, C.; Yu, J. Leader-following consensus of fractional-order multi-agent systems via adaptive pinning control. *Int. J. Control* **2015**, *88*, 1746–1756. [CrossRef]
8. Zhang, Y.; Wen, G.; Rahmani, A.; Peng, Z.; Hu, W. Cluster consensus of multi-agent systems with general linear and nonlinear dynamics via intermittent adaptive pinning control. *Trans. Inst. Meas. Control* **2020**, *43*, 014233122097525. [CrossRef]
9. Huang, D.; Jiang, H.; Yu, Z.; Hu, C.; Fan, X. Cluster-delay consensus in MASs with layered intermittent communication: A multi-tracking approach. *Nonlinear Dyn.* **2019**, *95*, 1713–1730. [CrossRef]
10. Yu, Z.; Sun, J.; Yu, S.; Jiang, H. Fixed-time consensus for multi-agent systems with objective optimization on directed detail-balanced networks. *Inf. Sci.* **2022**, *607*, 1583–1599. [CrossRef]
11. Sun, Y.; Li, W.; Zhao, D. Convergence time and speed of multi-agent systems in noisy environments. *Chaos* **2012**, *22*, 43126. [CrossRef] [PubMed]
12. Young, G.; Scardovi, L.; Leonard, N. Robustness of Noisy Consensus Dynamics with Directed Communication. In Proceedings of the American Control Conference, Baltimore, MD, USA, 30 June–2 July 2010; pp. 6312–6317.
13. Bamieh, B.; Jovanovi, M.R.; Mitra, P.; Patterson, S. Coherence in large-scale networks: Dimension-dependent limitations of local feedback. *IEEE Trans. Autom. Control* **2012**, *57*, 2235–2249. [CrossRef]
14. Patterson, S.; Bamieh, B. Consensus and Coherence in Fractal Networks. *IEEE Trans. Control Netw. Syst.* **2014**, *1*, 338–348. [CrossRef]
15. Patterson, S.; Yi, Y.; Zhang, Z. A Resistance-Distance-Based Approach for Optimal Leader Selection in Noisy Consensus Networks. *IEEE Trans. Control Netw. Syst.* **2018**, *6*, 191–201. [CrossRef]
16. Yi, Y.; Zhang, Z.; Shan, L.; Chen, G. Robustness of First-And Second-Order Consensus Algorithms for a Noisy Scale-free Small-World Koch Network. *IEEE Trans. Control Syst. Technol.* **2016**, *25*, 342–350. [CrossRef]
17. Sun, W. Coherence in a family of tree networks with an application of Laplacian spectrum. *Chaos* **2014**, *24*, 043112. [CrossRef] [PubMed]
18. Sun, W.; Li, Y.; Liu, S. Noisy consensus dynamics in windmill-type graphs. *Chaos* **2020**, *30*, 123131. [CrossRef] [PubMed]
19. Sun, W.; Hong, M.; Liu, S.; Fan, K. Leader-follower coherence in noisy ring-trees networks. *Nonlinear Dyn.* **2020**, *102*, 1–9. [CrossRef]
20. Wang, X.; Xu, H.; Dai, M. First-order network coherence in 5-rose graphs. *Physic A* **2019**, *527*, 121129. [CrossRef]
21. Huang, D.; Zhu, J.; Yu, Z.; Jiang, H. On Consensus Index of Triplex Star-Like Networks: A Graph Spectra Approach. *Symmetry* **2021**, *13*, 1248. [CrossRef]
22. Wan, Y.; Namuduri, K.; Akula, S.; Varanasi, M. The impact of multi-group multi-layer network structure on the performance of distributed consensus building strategies. *Int. J. Robust. Nonlinear Control* **2012**, *23*, 653–662. [CrossRef]
23. Wang, X.F. Complex netwroks, topology, dynamics and synchronization. *Int. J. Bifurc. Chaos* **2002**, *12*, 885–916. [CrossRef]
24. Chen, G.; Duan, Z. Network synchronization analysis: A graph-theoreic approach. *Chaos* **2008**, *18*, 037102. [CrossRef] [PubMed]
25. He, W.; Chen, G.; Han, Q.-L.; Du, W.; Cao, J.; Qian, F. Multiagent Systems on Multilayer Networks: Synchronization Analysis and Network Design. *IEEE Trans. Syst. Man Cybern. Syst.* **2017**, *47*, 1655–1667. [CrossRef]
26. Kivela, M.; Arenas, A.; Barthelemy, M.; Gleeson, J.P.; Moreno, Y.; Porter, M.A. Multilayer Networks. *J. Complex Netw.* **2014**, *2*, 203. [CrossRef]
27. Wang, Z.; Xia, C.; Chen, Z.; Chen, G. Epidemic Propagation With Positive and Negative Preventive Information in Multiplex Networks. *IEEE Trans. Cybern.* **2021**, *51*, 1454–1462. [CrossRef] [PubMed]
28. Lahby, M.; Essouiri, A.; Sekkaki, A. A novel modeling approach for vertical handover based on dynamic k-partite graph in heterogeneous networks. *Digit. Commun. Netw.* **2019**, *5*, 297–307. [CrossRef]
29. Xue, Y.; Yang, B.; Zhong, F.; Zilles, S. The Fast Search Number of a Complete k-Partite Graph. *Algorithmica* **2018**, *80*, 3959–3981. [CrossRef]
30. Li, Z. Exact Recovery of Community Detection in k-Partite Graph Models with Applications to Learning Electric Potentials in Electric Networks. *J. Stat. Phys.* **2021**, *182*, 6. [CrossRef]
31. Yang, F.; Jia, Z.; Deng, Y. Eigenvalue Spectrum and Synchronizability of Two Types of Double-Layer Star-Ring Networks with Hybrid Directional Coupling. *Discret. Dyn. Nat. Soc.* **2021**, *2021*, 6623648. [CrossRef]
32. Wang, L.; Jia, X.; Pan, X.; Xia, C. Extension of synchronizability analysis based on vital factors: Extending validity to multilayer fully coupled networks, Chaos. *Solitons Fractals* **2021**, *142*, 110484. [CrossRef]
33. Xu, M.M.; Lu, J.A.; Zhou, J. Synchronizability and eigenvalues of two-layer star networks. *Acta Phys. Sin.* **2016**, *65*, 028902.
34. Cvetkovic, D.; Rowlinson, P.; Simic, S. *An introduction to the Theory of Graph Spectra*; Cambridge University Press: Cambridge, UK, 2010.
35. Khalifeh, M.H.; Yousefi-Azari, H.; Ashrafi, A.R. The hyper-Wiener index of graph operations. *Comput. Math. Appl.* **2008**, *56*, 1402–1407.
36. Zhang, Z.; Zhu, Y. Cyclic arc-connectivity in a Cartesian product digraph. *Appl. Math. Lett.* **2010**, *23*, 796–800. [CrossRef]
37. Barik, S.; Pati, S.; Sarma, B. The Spectrum of The Corona of Two Graphs. *SIAM J. Discret. Math.* **2007**, *21*, 47–56. [CrossRef]
38. Liu, Q. The Laplacian spectrum of corona of two graphs. *Kragujev. J. Math.* **2014**, *38*, 163–170. [CrossRef]

39. Zhang, H.; Yang, Y. Resistance Distances and Kirchhoff index in circulant graphs. *Int. J. Quantum Chem.* **2007**, *107*, 330–339. [CrossRef]
40. Yang, Y.; Yu, Y. Resistance Distances and Kirchhoff indices under graph operations. *IEEE Access* **2020**, *8*, 95650–95656. [CrossRef]
41. Liu, Q.; Liu, J.; Cao, J. The Laplacian polynomial and Kirchhoff index of graphs based on R-graphs. *Neurocomputing* **2016**, *177*, 441–446. [CrossRef]
42. Liu, J.; Pan, X. A unified approach to the asymptotic topological indices of various lattices. *Appl. Math. Comput.* **2015**, *270*, 62–73. [CrossRef]
43. Li, X.; Peng, D. Extremal problems for graphical function-indices and f-weighted adjacency matrix. *Discrete Math. Lett.* **2022**, *9*, 57–66.

Disclaimer/Publisher's Note: The statements, opinions and data contained in all publications are solely those of the individual author(s) and contributor(s) and not of MDPI and/or the editor(s). MDPI and/or the editor(s) disclaim responsibility for any injury to people or property resulting from any ideas, methods, instructions or products referred to in the content.